ACES
DOI: 10.1002/asia.201500765
CHEMISTRY
AN ASIAN JOURNAL
Full Paper

RNA Modification

Chimeric RNA Oligonucleotides with Triazole and Phosphate Linkages: Synthesis and RNA Interference

Tomoko Fujino,[a] Kanako Kogashi,[a] Koudai Okada,[a] Martin Mattarella,[a] Takeru Suzuki,[a] Kenichi Yasumoto,[b] Kazuhiro Sogawa,[b] and Hiroyuki Isobe*[a, c]

Abstract: Chimeric RNA oligonucleotides with an artificial triazole linker were synthesized using solution-phase click chemistry and solid-phase automated synthesis. Scalable synthesis methods for jointing units for the chimeric structure have been developed, and after click-coupling of the jointing units with triazole linkers, a series of chimeric oligonucleotides was prepared by utilizing the well-established phosphoramidite method for the elongation. The series of chimeric 21-mer oligonucleotides that possessed the triazole linker at different strands and positions allowed for a screening study of the RNA interference to clarify the preference of the triazole modifications in small-interfering RNA molecules.

Introduction

Analogues of oligonucleotides are both attractive synthetic targets for chemists and interesting tools for biologists. Phosphate-replaced analogues that possess furanose-mimicking rings are particularly interesting because they can serve as substrates for enzymatic reactions despite their inertness toward nuclease hydrolysis.[1,2] Because of the robust elongation reactions of the so-called click chemistry,[3] triazole-linked DNA analogues (^{TL}DNA) have fulfilled the criterion for oligomer synthesis[2,4] and have proven useful in several enzymatic reactions.[5,6] Recently, we introduced an RNA analogue with triazole linkages (^{TL}RNA) by designing an elongation unit that possesses 3′-azido and 5′-acetylene moieties (Figure 1).[7,8] The synthetic access to this elongation unit was far superior to that of ^{TL}DNA because of the concise synthesis route from D-xylose as well as the selective and easy process for the nucleobase introduction, which allowed for the synthesis of oligomers.[2,9] However, exploration of the biological functions of the ^{TL}RNA oligomers was severely hampered by the poor solubility of the fully modified, electroneutral oligonucleotides. Therefore, we decided to incorporate the triazole linkages in the form of chimeric RNA oligonucleotides with a combination of natural, charged phosphate linkages. Scalable synthesis methods for jointing units for the chimeric structure have been developed, and after click-coupling of the jointing units with triazole linkers, a series of chimeric oligonucleotides was prepared by utilizing the well-established phosphoramidite method for the elongation.[10] The series of chimeric oligonucleotides that possess the triazole linkage at different positions provided us with a screening study of the RNA interference (RNAi) to clarify the tolerance of the triazole modifications in small interfering RNA (siRNA).[11,12]

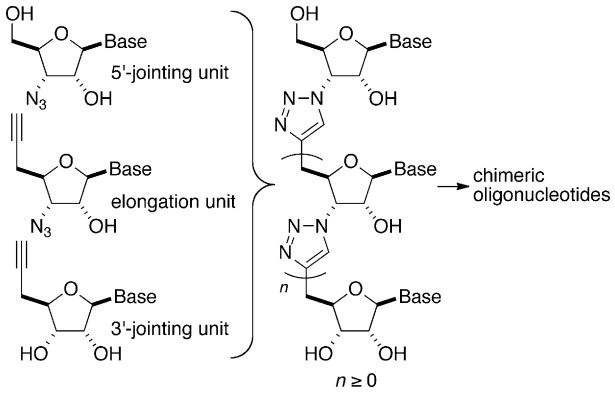

Figure 1. Structures of the triazole-linked RNA for the chimeric oligonucleotides.

[a] Dr. T. Fujino, K. Kogashi, K. Okada, Dr. M. Mattarella, T. Suzuki, Prof. H. Isobe
Department of Chemistry
Tohoku University
Aoba-ku, Sendai, 980-8578 (Japan)
E-mail: isobe@m.tohoku.ac.jp

[b] Dr. K. Yasumoto, Prof. K. Sogawa
Department of Biomolecular Sciences
Tohoku University
Aoba-ku, Sendai, 980-8578 (Japan)

[c] Prof. H. Isobe
JST, ERATO, Isobe Degenerate π-Integration Project and Advanced Institute for Materials Research
Tohoku University
Aoba-ku, Sendai, 980-8577 (Japan)

Supporting information for this article is available on the WWW under http://dx.doi.org/10.1002/asia.201500765.

Results and Discussion

Similar to the elongation units for the ^{TL}RNA,[7] synthesis routes from the readily available D-xylose were developed for the 5′- and 3′-jointing units. Because the synthesis routes intrinsically follow the preceding transformation processes, we briefly describe the design principles for each unit and provide the entire synthesis methodology in the Supporting Information. The 5′-jointing unit requires protecting groups on the nucleobases and on the 2′-OH and 5′-OH moieties, and it requires the 3′-azido group. Furthermore, the automated protocols for the phosphoramidite elongation required the presence of the 4,4′-dimethoxytrityl (DMTr) group on the 5′-OH moiety (see below). Thus, a series of compounds **1** that possessed four different nucleobases (U, C, A and G) was synthesized from D-xylose in high yields (Figure 2; see also Scheme S1 in the Supporting Information). The 3′-jointing unit requires protecting groups on the nucleobases, on the 2′-OH moiety, and on the acetylene unit at the 5′-position, and it requires a free 3′-OH moiety. Because of a potential cyclization reaction that can bridge the 2′- and 3′-OH groups, the protecting group for the 2′-OH was requisitely a silyl protecting group.[13] Therefore, compound **2** was designed and synthesized with four different nucleobases (U, C, A and G) in high yields (Figure 2; see also Scheme S2).

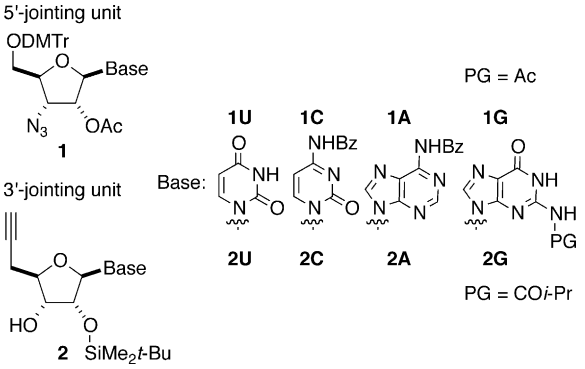

Figure 2. The jointing units synthesized in this study.

The two jointing units were coupled to produce the simplest triazole-linked dinucleotides for examination in the automated phosphoramidite protocols ($n=0$, Figure 1). Among the 16 possible structures for the dinucleotides, we selected three representative examples from a combination of pyrimidines for this first study. As shown in Scheme 1, we coupled **1** and **2** by a copper-catalyzed Hüisgen [3+2] cycloaddition reaction and subsequently converted the dinucleotides into phosphoramidites. The yields were moderate to good for the two-step transformation, and three dinucleotides, **U*t*U**, **C*t*U** and **C*t*C**, were synthesized in 87%, 77% and 80% yields, respectively.

We incorporated the triazole-linked dinucleotide in a 21-mer oligonucleotide with an siRNA sequence to target a gene of enhanced yellow-fluorescent protein (EYFP).[14] Using dimers in our hands, we designed two siRNA, siRNA-a and siRNA-b (Scheme 2), for the EYFP target gene and synthesized 13 oligonucleotides varying the positions of modification.[11] The location of target sites in the EYPF gene are shown in Figure S52. For siRNA-a, oligonucleotide **7** possessed a sequence for a passenger strand, and oligonucleotide **8** possessed a sequence for a guide strand. For siRNA-b, oligonucleotide **9** was the passenger strand, and oligonucleotide **10** was the guide strand.

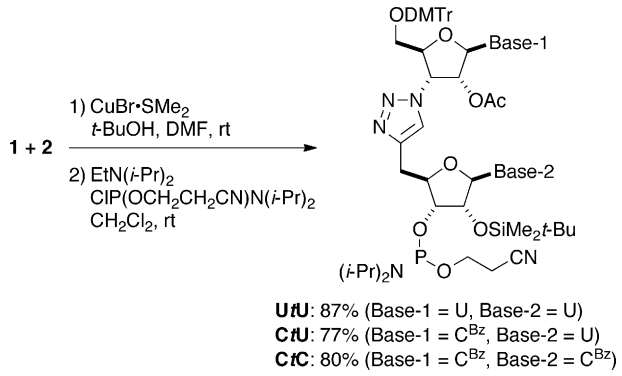

Scheme 1. Synthesis of the triazole-linked dinucleotides. The triazole linkage is represented as ***t***.

The triazole-linked dinucleotide was incorporated using the phosphoramidite method that was executed on an automated synthesizer (M-2-MX, Nihon Techno Service) with controlled pore glass (CPG) beads, and the representative steps for the incorporation are shown in Scheme 2. For the 3′-jointing process for the initial chimeric structure **4**, the phosphoramidite end of the dinucleotide was activated with 5-benzylthio-1*H*-tetrazole (BTT) to couple with the hydroxy end either of a nucleoside or of a universal linker[15] on the CPG beads. The subsequent processes were identical to those for the standard phosphoramidite protocol[10] and involved capping of the unreacted hydroxy ends, oxidation of the phosphorous moieties and deprotection of the 5′-end DMTr group. For the 5′-jointing process to elongate the natural nucleotides, the standard phosphoramidite method was adopted with the natural nucleoside **5**, which was repeated to complete the desired sequence. The efficiency of elongation was tracked for each step with an LED detector implemented on the synthesizer and was finally determined at the final detritylation process using the standard protocol to quantify the trityl cation on a UV/Vis spectrometer. The synthesis of the 21-mer involved 19/20 elongation steps and, as shown in Scheme 2, the presence of the triazole-linkages did not affect the efficiency: the total yields of the oligonucleotides ranged from 30% to 60%, which required very high efficiencies of 94–97% per one elongation step.

Finally, the activity of the chimeric oligonucleotides as siRNA was examined. We assembled the double-stranded siRNA by combining the passenger strand (**7** or **9**) and the guide strand (**8** or **10**)[16] and introduced it into HeLa cells. A plasmid pEYFP-N1 with the target EYFP gene was also transfected with a plasmid pTagRFP-C that carried a reference gene of red fluorescent protein (tagRFP) as the internal standard. The reduction in the target EYFP expression was quantified by quantitative RT-PCR of the corresponding mRNA in comparison with the standard tagRFP expression (see the Experimental Section for the detailed procedures).[5,17]

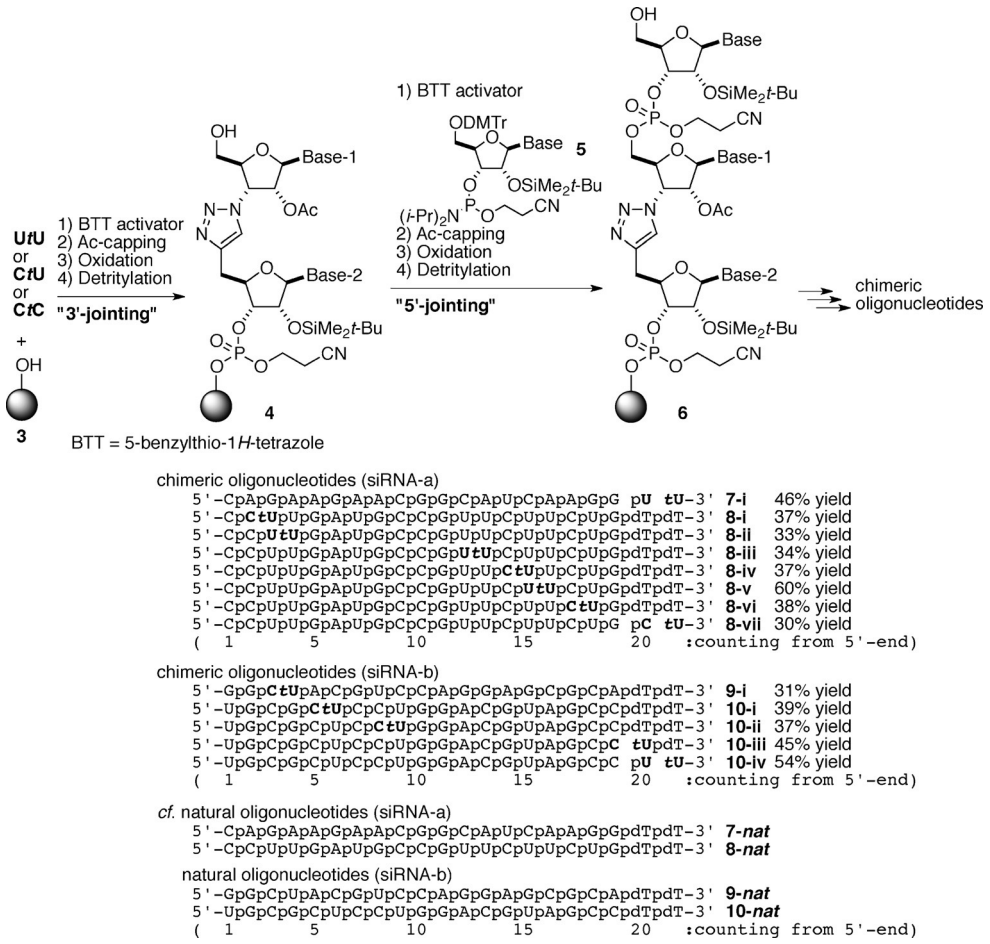

Scheme 2. Synthesis of 21-mer oligonucleotides for the RNAi assay.

The sequences of siRNA-a and siRNA-b were selected so that we could cover a variety of modification sites with our pyrimidine dimers. Note that modifications in the guide strand of the siRNA are regarded as more challenging,[12] and we examined a larger number of variants in the guide strand. The locations of the triazole modifications in terms of counting from the 5′-end in siRNA were 2–3, 3–4, 12–13, 14–15, 15–16, 17–18 and 20–21 for the guide strand **8** in siRNA-a and 5–6, 8–9, 19–20 and 20–21 for the guide strand **10** in siRNA-b. The oligonucleotides were screened for the siRNA activity via two stages, and, at the first stage, a rough screening of modification sites was executed by a single-set experiment for 13 oligonucleotides. As shown in Figure S53, most of the modifications in RNA-a were not tolerated except the 3′-overhang region at the 20–21 counting with **7-i**/**8-vii** combination. Note that the examination of the 3′-overhang region was also included in RNA-b and that the in-depth evaluation was performed with RNA-b (see below). At the second stage, we further accumulated data for potent candidates (RNA-b) in the first stage with experiments being executed in triplicate to obtain reliable and quantitative data for the positive experiments (Figure 3).

As is typical with artificial oligonucleotides,[12d–f] the modification in the passenger strand was well tolerated to achieve siRNA activity, and the passenger strand **9-i** with a triazole modification at 3–4 counting from the 5′-end interfered the target gene at 7% expression level. This interference level was comparable with that of the siRNA-b with natural oligonucleotide **9-*nat*** of 4% expression level. As was the case with RNA-a, the triazole linkers were favorably tolerated in the downstream region, and modifications in the 3′-overhang regions at 19–20 and 20–21 counting from the 5′-end with **9-iii** and **9-iv** suppressed the expression levels to 10% and 6%, respectively. Because the interference with the **7-i**/**8-vii** combination (Figure S53) was not more potent than those of **9-i**/**10-*nat*** or **9-*nat*/10-iv** combinations, the chimera/chimera combination of two modified oligonucleotides with a triazole linker may not be effective for a synergetic improvement of interference.[12d–f] However, the modifications in the upstream region considerably affected the siRNA activity. The oligonucleotide **10-i** exhibited negligible interference activity. The triazole modification in this oligonucleotide was located between nucleotides of 5–6 counting from the 5′-end. This region of 2–8 counting from the 5′-end is known as the seed region where the hydrogen bonding from the Argonaute protein captures the phosphate groups[18] and the complementarity of base pairing with the target strand plays a crucial role for the siRNA activity.[12] The oligonucleotide **10-ii** with the triazole modification between nucleotides of 8–9 counting from the 5′-end indeed exhibited a moderate level of interference and suppressed the expression to 46%. A dose dependency of the siRNA activities was evaluated with the most potent chimeric siRNA of **9-*nat*/10-iv**. As shown in Figure 3b, the influence of the concentration on the interference was more apparent with **9-*nat*/10-iv** than the natural combination of **9-*nat*/10-*nat***.

Finally, Figure 4 shows the results of analysis of the translated products by fluorescent microscopy. A comparison of tagRFP with 4′,6-diamidino-2-phenylindole (DAPI) shows the transfection efficiency of the plasmids with marker genes, and a comparison of EYFP with tagRFP shows the RNAi activity. A further comparison of EYFP in control with those in **9-*nat*/10-*nat*** or **9-*nat*/10-iv** clarifies the RNAi activities of the chimeric siRNA. The chimeric siRNA **9-*nat*/10-iv** indeed suppressed the production of the target EYFP at the level comparable to the natural congener **9-*nat*/10-*nat***, which is consistent with the results from quantitative PCR analysis. The results confirmed that

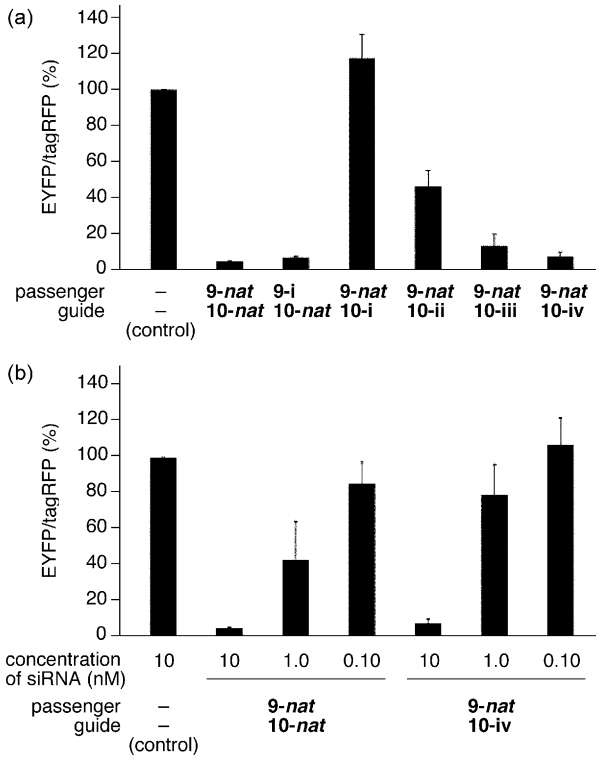

Figure 3. Performance of the siRNA as measured by EYFP gene expression in HeLa cells in comparison with the RFP gene as the internal standard. Average data with error bars from triplicate runs are shown. (a) Dependency of siRNA activities on the triazole modification positions at the concentration of 10 nM of siRNA. (b) Dependency of siRNA activities on the concentrations as measured with the most potent siRNA-b (**9-*nat*/10-iv**). The total concentration of transfected RNAs was maintained at 10 nM, and the additional non-targeting RNA was introduced for the experiments with siRNA below 10 nM.

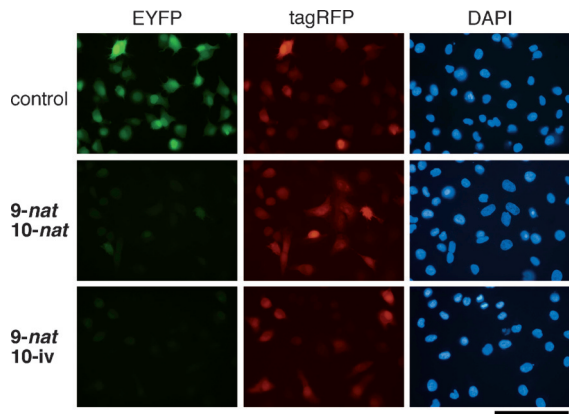

Figure 4. Fluorescent microscopy images for the translated products of EYPF (green) and tagRFP (red). Two siRNA, **9-*nat*/10-*nat*** and **9-*nat*/10-iv**, target the EYFP gene. Images (blue) with DAPI staining for non-selective, nuclear staining are also shown. A control experiment was carried out with non-targeting RNA, and a reference experiment was carried out with natural siRNA **9-*nat*/10-*nat***. The experiment with chimeric siRNA **9-*nat*/10-iv** showed a comparable suppression of EYFP production with the natural reference via RNAi. The images shown are representative of three independent experiments. Scale bar, 100 μm.

the chimeric RNA oligonucleotide possessing a triazole linkage functioned as siRNA and, albeit depending on the installed positions, that the silencing activities could compete with the natural RNA oligonucleotides.

Conclusions

In summary, we have developed a concise synthesis method for nucleoside analogues that serves as jointing units for chimeric RNA oligonucleotides with triazole linkages. In total, 48 compounds including 13 chimeric oligonucleotides were newly synthesized. In combination with four elongation units,[7] eight jointing units that possess four different nucleobases can provide a synthesis route to any sequence of oligonucleotides with triazole linkages at any desired position. Note that the method allows for the introduction of non-natural nucleobases through glycosidation reaction with the corresponding nucleobase units. The present study also demonstrates the applicability of the triazole-linked nucleotides for the automated protocols of phosphoramidite methods, which allow for the incorporation of the triazole linker in 21-mer oligonucleotides for siRNA. The chimeric oligonucleotides were examined for the RNAi activity, and we revealed the preference of the triazole modifications, which added a new, synthetically viable entry into the rapidly growing library of siRNA variants.[12] We believe that the present synthesis method will lead to the development of various functional RNA molecules in the future.

Experimental Section

General

All the reactions were carried out under an inert atmosphere of nitrogen unless otherwise noted. Analytical thin-layer chromatography (TLC) was performed on a glass plate coated with silica gel (230–400 mesh, 0.25 mm thickness) containing a fluorescent indicator (silica gel $60F_{254}$, Merck). Flash silica gel column chromatography was performed on 60N (spherical and neutral gel, 40–50 μm, Kanto).[19] Elongation of chimeric oligonucleotides was performed on a Nihon Techno Service M-2-MX DNA/RNA synthesizer. Analysis of reaction mixtures with high pressure liquid chromatography (HPLC) were performed on HPLC systems equipped with ODS column (COSMOSIL C18-MS-II, 4.6×250 mm, Nacalai Tesque; column temperature 40 °C), and purification of products was performed with ODS column (COSMOSIL C18-MS-II, 20×250 mm, Nacalai Tesque). IR spectra were recorded on NICOLET iS10 equipped with an attenuated total reflection (ATR; powder) and were reported as wavenumbers (ν) in cm^{-1}. Proton (^1H) and carbon (^{13}C) nuclear magnetic resonance (NMR) spectra were recorded on JEOL JNM-ECS 400 (^1H: 400 MHz; ^{13}C: 100 MHz; ^{31}P: 160 MHz) spectrometers. Methyl (CH_3), methylene (CH_2) and methyne (CH) signals in ^{13}C NMR spectra were assigned by DEPT spectra. ^1H NMR spectra and ^{13}C NMR spectra in $CDCl_3$ were referenced to the solvent resonances, and ^{31}P NMR spectra were referenced to 85% H_3PO_4 as an external standard. High resolution mass spectra were obtained on JEOL JMS-T100 LC or SolariX 9.4T instrument (ESI-TOF MS) with reserpine (1 ng μL^{-1}) and a mixture of polyethylene glycol (PEG200 20 ng, PEG600 20 ng, PEG1000 30 ng, PEG2000 60 ng in 1 μL) as an internal standard. A molar amount of trityl cation at the final elongation step was quantified on a UV-visible spectrometer (JASCO, V-

670) to determine the elongation efficiencies. Thermal melting curve was also obtained on the spectrometer equipped with a water-circulated temperature-controlled cell holder (JASCO, ETC-717). The melting temperature was determined using a melting program (JASCO, VWTP-780). Quantitative PCR was performed on ABI 7300 Real Time PCR System (Applied Biosystems), and the levels of PCR products were analyzed with 7300 System SDS software (Applied Biosystems). Fluorescent microscopic analysis was performed by using an Olympus IX-71 system equipped with color filters of U-MYFPHQ (EYFP), U-MRFPHQ (tagRFP) and U-MWU2 (DAPI) on an Olympus DP70 CCD camera.

Materials

Anhydrous THF (stabilizer free, Kanto), DMF (dehydrated, Kanto) and toluene (dehydrated, Kanto) were purified by using a solvent purification system (GlassContour) equipped with columns of activated and supported copper catalyst (Q-5). Water was purified by using a Milli-Q ultrapure water system (Millipore). Other solvents were purified by distillation and dried over 4 Å molecular sieves. D-Xylose, triflic acid, sodium azide, *N*,*N*-dimethyl-4-aminopyridine (DMAP), pyridinium dichromate (PDC), (triisopropylsilyl)acetylene, uracil, *N*,*O*-bis(trimethylsilyl)acetamide, 9-acetyl-2-(acetylamino)-6,9-dihydro-1*H*-purin-6-one, triethylamine, Eagle's minimal essential medium (E-MEM) and penicillin-streptomycin solution were purchased from Wako, and triethylamine was purified by distillation before use. Benzyl bromide, sodium borohydride and *tert*-butyllithium were obtained from Kanto, and *tert*-butyllithium was titrated before use. Triflic anhydride, hexamethyldisilazane, trimethylsilyl triflate, boron trichloride, *n*-tetrabutylammonium fluoride, *tert*-butyldimethylsilyl chloride, imidazole and cytosine were purchased from TCI. *n*-Tetrabutylammonium iodide, adenine, benzoyl cytosine, primers, DAPI and fluorescein amidite (FAM)-labeled Taqman probes used for quantitative PCR were purchased from Aldrich. Diisopropylethylamine, trimethylsilyl chloride, dimethoxytrityl chloride, boron trifluoride diethyl etherate, isobutyryl chloride and paraformaldehyde were purchased from Nacalai Tesque. β-Cyanoethyl 2′-*O*-TBDMS RNA phosphoramidites, Glen UnySupport 500 and other reagents for oligonucleotide synthesis were purchased from Glen Research. Solid supports (dT-CPG 500 and 5′-DMT-Suc-CPG 500) loaded with dT were purchased from Glen Research and Biosearch technologies. Sep-Pak column (tC18 pPlus short cartridge, 37–55 μm) was purchased from Waters. Natural 21-mer oligonucleotides were purchased from Hokkaido System Science, and 4-(2-hydroxyethyl)-1-piperazineethanesulfonic acid-potassium hydroxyde (HEPES-KOH) buffer was purchased from JBioS. Fetal bovine serum (FBS) was purchased from BioWest. pEYFP-N1 plasmid, Prime Script RT reagent Kit (Perfect Real Time) and Premix Ex Taq were purchased from Takara, and pTagRFP-C was purchased from Evrogen. Lipofectamine 2000 and TURBO DNase were purchased from Life Technologies. ISOGEN was purchased from NIPPON GENE. Phosphate-buffered saline (PBS) was purchased from Nissui. Fluorescence mounting medium was purchased from DAKO.

Synthesis

See the Supporting Information for the procedures and spectral data.

Formation of siRNA duplex for RNAi

A mixture of a passenger strand **7** (20 μM) and a guide strand **8** (20 μM) in HEPES-KOH buffer (30 mM, pH 7.4) containing potassium acetate (100 mM) and magnesium acetate (10 mM) was heated at 90 °C for 1 min and allowed to cool to 30 °C over a period of 25 min. The structures of siRNA were shown in main text. For a negative control, non-targeting RNA duplex with 5′-CpGpApApUpCpC-pUpApCpApApApGpCpGpCpGpCpdTpdT-3′ and 5′-GpCpGpCpGpCpUpUpUpGpUpApGpGpApUpUpCpGpdTpdT-3′ was prepared.

RNAi experiments

HeLa cells were cultured in E-MEM supplemented with 10% v/v FBS and 1% v/v penicillin-streptomycin at 37 °C with 5% CO_2,[11] and the growing cells in E-MEM with 10% v/v FBS (1.5×10^5 cells mL^{-1}) were plated into each well of 12-well plates (1 mL/well) and incubated for 24 h prior to transfection. The cells were then transfected with a mixture of pEYFP-N1 plasmid (0.15 μg), pTagRFP-C plasmid (0.15 μg) and siRNA duplex (10 pmol) using lipofectamine 2000 (2.0 μL). After 4 h, the medium was exchanged with fresh growth medium containing 10% v/v FBS. The cells were allowed to grow for 48 h and the gene expression levels were analyzed by quantitative RT-PCR and fluorescent microscopy in terms of mRNA transcripts and translated proteins, respectively.

Quantification of RNAi activity with RT-PCR

Gene expression in terms of mRNA transcripts was quantified by quantitative RT-PCR, and the RNAi activity was evaluated as an interfered level of the EYFP expression that was quantified relative to the tagRFP expression as an internal reference.[17] The relative expression value was further standardized by the value from the negative control (see above) to afford the EYPF/tagRFP value in percentage (Figure 3). The total RNA was extracted from HeLa cells using ISOGEN (200 μL) and was treated with DNase (TURBO DNase, 4 U). The total RNA (0.5 μg) was transcribed to cDNA using the PrimeScript RT reagent kit (Perfect Real Time), and 1/25th of cDNA solution was subjected to PCR with PremixEx Taq (10 μL) in the presence of a primer (0.2 μM) and a TaqMan probe (0.1 μM). For EYFP analysis, the primers were 5′-d(CpCpApCpTpApCpCpApGpCpApG-pApApCpApCpCpC)-3′ and 5′-d(CpTpCpGpTpTpGpGpGpGpTpCpTpTpTpGpCpTpCpApG)-3′, and the TaqMan probe was 5′-FAM-d(TpGpCpTpGpCpTpGpCpCpGpApCpApApCpCpApCpT-pApCpCpT)-TAMRA-3′. For tagRFP analysis, the primers were 5′-d(CpTpGpGpCpTpApCpCpApGpCpTpTpCpApTpGpTpApCpG)-3′ and 5′-d(CpCpCpTpCpApGpGpGpApApGpGpApCpTpGpCpTpTpA)-3′, and the TaqMan probe was 5′-FAM-d(ApGpCpApGpA-pApCpCpTpTpCpApTpCpApApCpCpApCpApCpCpCpApGpG)-TAMRA-3′. The PCR was carried out, after heat treatment at 95 °C for 3 min, by 40 cycles of 95 °C for 15 s and 60 °C for 1 min on an ABI 7300 Real Time PCR System. The RNAi experiments were carried out at least in duplicate, and the average values are shown in Figure 3.

Qualitative analysis of RNAi activity with fluorescent microscopy

Gene expression in terms of translated proteins was imaged by fluorescent microscopy. The siRNA experiments were performed on a cover glass embedded in the well for translocation. The cells were washed with PBS, fixed with 4% v/v paraformaldehyde/PBS for 15 min and stained with DAPI (0.2 μg mL^{-1} in PBS) for 10 min. The slide glass was wetted with fluorescence mounting medium, and the cover glass with cells was translocated. Marker proteins of EYFP and tagRFP were imaged with an exposure time of 0.5 s, and DAPI stains were imaged with an exposure time of 0.05 s.

Acknowledgements

This work was partly supported by KAKENHI (26810083).

Keywords: click chemistry · oligonucleotides · RNA · siRNA · solid-phase synthesis

[1] E. Uhlmann, A. Peyman, *Chem. Rev.* **1990**, *90*, 543 – 584.
[2] H. Isobe, T. Fujino, *Chem. Rec.* **2014**, *14*, 41 – 51.
[3] a) M. Meldal, C. W. Tornøe, *Chem. Rev.* **2008**, *108*, 2952 – 3015; b) H. C. Kolb, K. B. Sharpless, *Drug Discovery Today* **2003**, *8*, 1128 – 1137.
[4] a) H. Isobe, T. Fujino, N. Yamazaki, M. Guillot-Nieckowski, E. Nakamura, *Org. Lett.* **2008**, *10*, 3729 – 3732; b) T. Fujino, N. Yamazaki, H. Isobe, *Tetrahedron Lett.* **2009**, *50*, 4101 – 4103; c) T. Fujino, N. Yamazaki, A. Hasome, K. Endo, H. Isobe, *Tetrahedron Lett.* **2012**, *53*, 868 – 870.
[5] T. Fujino, K. Yasumoto, N. Yamazaki, A. Hasome, K. Sogawa, H. Isobe, *Chem. Asian J.* **2011**, *6*, 2956 – 2960.
[6] a) A. H. El-Sagheer, A. P. Sanzone, R. Gao, A. Travassoli, T. Brown, *Proc. Natl. Acad. Sci. USA* **2011**, *108*, 11338 – 11343; b) A. P. Sanzone, A. H. El-Sagheer, T. Brown, A. Tavassoli, *Nucleic Acids Res.* **2012**, *40*, 10567 – 10575; c) C. N. Birts, A. P. Sanzone, A. H. El-Sagheer, J. P. Blaydes, T. Brown, A. Tavassoli, *Angew. Chem. Int. Ed.* **2014**, *53*, 2362 – 2365; *Angew. Chem.* **2014**, *126*, 2394 – 2397; d) A. H. El-Sagheer, T. Brown, *Acc. Chem. Res.* **2012**, *45*, 1258 – 1267.
[7] T. Fujino, K. Endo, N. Yamazaki, H. Isobe, *Chem. Lett.* **2012**, *41*, 403 – 405.
[8] Although its bond periodicity does not mimic the natural six-bond periodicity, one example of chimeric RNA with a triazole linker has been reported: D. Mutisya, C. Selvam, S. D. Kennedy, E. Rozners, *Bioorg. Med. Chem. Lett.* **2011**, *21*, 3420 – 3422.
[9] For instance, we synthesized a 10-mer oligonucleotide with 5′-A*t*C*t*G*t*U-*t*A*t*G*t*C*t*C*t*dT*t*dT-3′ sequence (ref. 2), aiming at an siRNA molecule, but failed in further extension due to the extremely low solubility.
[10] M. H. Caruthers, *Acc. Chem. Res.* **1991**, *24*, 278 – 284.
[11] C. Li, P. D. Zamore in *Molecular Cloning, A Laboratory Manual, 4th ed., Vol. 3* (Eds.: M. R. Green, J. Sambrook), Cold Spring Harbor Laboratory Press, New York, **2001**, pp. 1415 – 1479.
[12] a) Y. Dorsett, T. Tuschl, *Nature* **2004**, *3*, 318 – 329; b) G. F. Deleavey, M. J. Damha, *Chem. Biol.* **2012**, *19*, 937 – 954; c) J. B. Bramsen, J. Kjems, *Front. Genet.* **2012**, *3*, 1 – 22; d) D. Mutisya, C. Selvam, B. D. Lunstad, P. S. Pallan, A. Haas, D. Leake, M. Egli, E. Rozners, *Nucleic Acids Res.* **2014**, *42*, 6542 – 6551; e) W. Gong, J.-P. Desaulniers, *Bioorg. Med. Chem. Lett.* **2012**, *22*, 6934 – 6937; f) T. C. Efthymiou, V. Huynh, J. Oentoro, B. Peel, J.-P. Desaulniers, *Bioorg. Med. Chem. Lett.* **2012**, *22*, 1722 – 1726.
[13] a) K. K. Ogilvie, N. Theriault, K. L. Sadana, *J. Am. Chem. Soc.* **1977**, *99*, 7741 – 7743; b) N. Usman, K. K. Ogilvie, M.-Y. Jiang, R. J. Cedergren, *J. Am. Chem. Soc.* **1987**, *109*, 7845 – 7854.
[14] a) B. P. Cormack, R. H. Valdivia, S. Falkow, *Gene* **1996**, *173*, 33 – 38; b) R. Y. Tsien, *Annu. Rev. Biochem.* **1998**, *67*, 509 – 544.
[15] V. Ravilkumar, M. Manoharan, A. P. Guzaev, Z. Wang, R. K. Kumar, U.S. Patent 7202264, **1995**.
[16] The duplex formation was confirmed by measuring the melting temperature (T_m) using UV/Vis spectroscopy. The T_m of the representative duplex between **8-ii** and ***7-nat*** in SSPE buffer (10 mM sodium phosphate (pH 7.0), 100 mM sodium chloride, 0.10 mM ethylenediamine tetraacetic acid) was observed at 82 °C that was slightly lower than the T_m of the control duplex between ***8-nat*** and ***7-nat*** (> 85 °C).
[17] P. C. Scacheri, O. Rozenblatt-Rosen, N. J. Caplen, T. G. Wolfsberg, L. Umayam, J. C. Lee, C. M. Hughes, K. S. Shanmugam, A. Bhattacharjee, M. Meyerson, F. S. Collins, *Proc. Natl. Acad. Sci. USA* **2004**, *101*, 1892 – 1897.
[18] a) Y. Wang, G. Sheng, S. Juranek, T. Tuschl, D. J. Patel, *Nature* **2008**, *456*, 209 – 213; b) E. Elkayam, C.-D. Kuhn, A. Tocilj, A. D. Haase, E. M. Greene, G. J. Hannon, L. Joshua-Tor, *Cell* **2012**, *150*, 100 – 110.
[19] W. C. Still, M. Kahn, A. Mitra, *J. Org. Chem.* **1978**, *43*, 2923 – 2925.

Manuscript received: July 22, 2015
Accepted Article published: August 6, 2015
Final Article published: August 26, 2015